13th International Conference on
Structural Health Monitoring of Intelligent Infrastructure
DOI: 10.3217/978-3-99161-057-1-082

Synthetic environment for close-range photogrammetry-based surface friction assessment of road infrastructures

Cheng Peng[1], Yi Jiang[1], Shuo Li[1, 2]
[1]School of Construction Management Technology, Purdue University, 363 N Grant St., West Lafayette, IN
[2]Division of Research and Development, Indiana Department of Transportation, 1205 Montgomery St., West Lafayette, IN
email: peng211@purdue.edu, jiang2@purdue.edu, sli@indot.in.gov

ABSTRACT: Quantification of friction demands is a major task in management of road infrastructures. The use of pavement texture measurement in friction assessment offers the potential for describing road frictional characteristic in a non-contact manner. However, surface macrotexture profiles tested by stationary measurements and high-speed laser systems provide limited range of texture information at high frequency scales. To achieve adequate outdoor road surface reconstruction at ultra-high resolution and low cost, this research develops a synthetic environment for ground truth reference and efficient generation of data and experiment. To illustrate the approach, a photo-realistic computer graphics model of asphalt pavement surface is produced and virtually scanned using candidate image acquisition plans. Then, in-depth quality assessment of the corresponding 3D point cloud reconstruction models is performed. In this way, suggest use of a close-range photogrammetric pavement surface scan method using Structure-from-Motion (SfM) technology and its requirements for friction-oriented texture quantification in terms of spatial resolution, camera movement, and illumination configuration is put forth. The effectiveness of the synthetic environment and the optimized experiment setup is demonstrated through a field survey on three roads. Finally, the obtained point cloud datasets are used in texture feature characterization and friction number prediction modeling processes.

KEY WORDS: Synthetic environment; Structure-from-Motion; Pavement texture measurements; Infrastructure friction performance.

1 INTRODUCTION

Pavement skid resistance is one of the most important properties among other highway surface characteristics. Demand for engineering interventions to restore friction of the aging and deteriorating highway network has been increased through years. Period assessment of pavement friction performance at the tire-road interaction has a pivotal role in developing the inventory of the condition of infrastructures at the highway network level. Current means of tire friction measurement devices and processes need calibration and harmonization for quality assurance. The use of pavement texture measurement in friction prediction offers the potential for describing highway frictional characteristic in a non-contact manner. To this end, such practices need to identify a comprehensive list of pavement macrotexture and microtexture attributes which contribute to friction. Both stationary measurements and high-speed laser systems are employed for sufficient reconstruction of macrotexture surface profiles [1]. However, a lower bound of microtexture wavelengths that relate to pavement skid resistance is not standardized. Furthermore, not all high frequency scales of microtexture are measurable. Criteria for sufficient spatial sampling rate and quality quantification of a pavement microtexture measurement approach, which includes all useful scales, is still vague [2].

In this paper, camera-based sensing of highway surface texture, using Structure-from-Motion (SfM) technique, is suggested for outdoor practices of high-resolution reconstruction of surface topography. In order to make fully use of the advantages provided by SfM technique while at the same time quantify and overcome limitations observed in previous studies, the investigation qualify SfM pipelines for pavement texture measurements with three main contributions: (1) in-depth quantitative studies of the texture measurement accuracy influenced by the photogrammetric capturing quality of highway surfaces at high frequency scales; (2) comprehensive list of 3D texture characteristics contributing to the texture-friction correlation; (3) suggest use of an experimental setup using commercial off-the-shelf camera and its requirements for sufficient pavement texture quantification in terms of spatial resolution, camera movement, and illumination configuration is put forth. The works aims to optimize the use of outdoor photogrammetry techniques to friction-oriented road surface assessment, particularly for sufficient characterization of surface texture at micro-scales.

2 PAVEMENT SYNTHETIC ENVIRONMENT

Development of a synthetic test environment for close-range image acquisition of pavement surface topography is important for the proposed investigation for two main reasons:

1. Ground truth measurement: Evaluation of the SfM surface reconstruction quality in terms of texture characterization requires a well-defined ground truth model as the target reference. More often, camera-based approaches rely on a comparison to model from another costly technique such as a laser texture scanner or a microscopy. Therefore, the quality of such a comparison is limited by inevitable uncertainty in the reference model. Practices to mitigate this drawback include replication molding of the target surface and the use of 3D-print target objects [3]. In an approach using synthetic environment, the surface topography ground truth data is available. The

DOI: 10.3217/978-3-99161-057-1-082

accuracy and quality of a SfM reconstructed surface digital elevation model (DEM) can be quantified using a direct comparison to the ground truth displacement map of the synthetic texture model. Subsequently, the pavement texture measurement performance from a photogrammetric survey can be optimized based on the observed variation in comparison results.

2. Efficient data generation and experiment: In the submillimetre, and micrometer range, quality of a photogrammetric surface reconstruction can be affected not only by the environmental and apparatus setups, but also by local characteristic variations of a target surface texture. Conducting a quantitative study of these factors in the field is time and cost consuming. In contrast, SfM surveys using images rendered in the synthetic environment can efficiently cover a wide variety of system configurations at any time without labor-intensive and site-sensitive field surveys.

A synthetic environment has been developed to test and quantify all influential factors regarding pavement macrotexture and microtexture measurements in a generalizable manner. To bring the close-range photogrammetric setup into the outdoor field environment, the image acquisition strategy should be developed, tested, and optimized for an efficient and robust performance.

Blender software is used to implement the synthetic modeling steps introduced herein. To extend the synthetic environment to a generalizable one, the high-resolution surface geometric details are modeled with a variation of texture characteristics using the Blender-Python API (Blender, 2024). The developed environment is used to produce survey images "captured" by a virtual micro-four thirds camera using different ground sampling distance (GSD). The resolution of each simulated image is 4592 × 3448, in which each pixel has a size of 3.77 μm. This section describes the detail of each created texture model and the steps to develop the synthetic setup for pavement close-range photogrammetric texture measurement. First, a mesh of each solid object in the environment is created to represent the 3D geometric details of the target structure. Then, multiple texture maps and settings are imported to control base color, roughness, and shading effects of the object surfaces. Third, a simplified surrounding scene is configured, and a camera-light pair is positioned facing down at a determined height. Finally, a group of simulated images rendered from predetermined viewpoints are produced. An overview of the development is depicted in Figure 1.

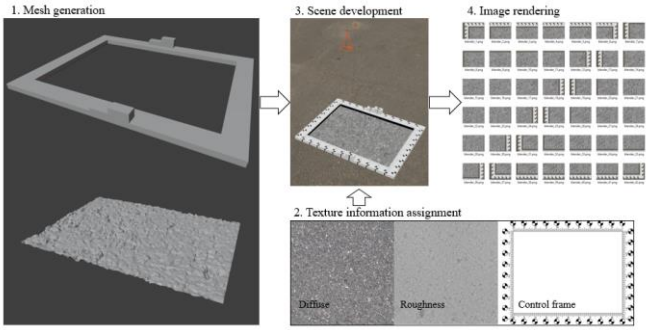

Figure 1. Framework for the synthetic approach of pavement texture photogrammetry.

2.1 Synthetic Data Generation

The synthetic environment developed in this research consists of a 100 mm x 75 mm patch of surface texture with four edges enclosed by a 10 mm wide rectangular control frame.

A solid object of control frame was generated in the synthetic environment. A cardboard thickness of 3.175 mm (1/16 in.) was selected to ensure flatness of reference surface for surveys in the field. The frame has a rectangular shape, and its inner and outer dimensions are 100 mm x 75 mm and 120 mm x 95 mm. The 10 mm width of four edges is selected so that the entire inner scanning area can be captured with at least two images (high overlapping). With a printed paper texture projected on the control frame top surface, a total of 40 reference marks of 5 mm diameter are horizontally distributed on the edges of the enclosed target scanning area. The edge distribution approach of ground control points (GCPs) is followed to have an optimized mapping accuracy [4] and to avoid texture occlusion. Previous studies have observed that the addition of a few vertically distributed GCPs can decrease the vertical reprojection error of a UAV surface mapping without influencing the planimetric accuracies [4], [5]. Therefore, additional heights (1/32 in., 1/16 in., 3/32 in., 1/8 in.) are added to four of the 40 edge marks so that they can be utilized as vertical GCPs.

A photogrammetry-based asphalt material downloaded from an public database [6] was adapted to generate a realistic pavement texture at a ultra-high level of resolution in the synthetic environment. The original data has a color map, a roughness map, a normal map, and a displacement map, each was represented by a 16K image of 1.2 m x 1.2 m area. Several data processing steps were developed to the texture maps so that realistic ground truth textures with a variation of statistical characteristics can be tested in the synthetic environment.

1. The original maps have a resolution of 186.4p/mm^2, equivalent to a pixel size of 73.2μm. Each of the three texture maps was refined to have an ultra-high resolution of 1.68Kp/mm^2 (24.41μm pixel size) using bicubic interpolation. The 3D surface developed from a refined texture mesh has a smooth mesh geometry in the simulated images, in which unexpected edge artifacts in the high-frequency domain become invisible to the virtual camera pixels. Figure 2 shows a 5cm x 5cm patch of the surface color map before and after the interpolation. While increasing the synthetic surface smoothness enables a more realistic modeling of structure, it significantly increases the required computational power and time. The increased resolution of 1.68Kp/mm^2 in the geometry modeling of ground truth surfaces is selected to offer a tradeoff between model reality and tedious work. As a result, the ground truth power spectrum density (PSD) has a nominal high cutoff wavevector of:

$$\frac{2\pi}{\lambda_{min}} = \frac{2\pi}{4.882\times10^{-5}m} = 1.287 \times 10^5 m^{-1} \quad (1)$$

DOI: 10.3217/978-3-99161-057-1-082

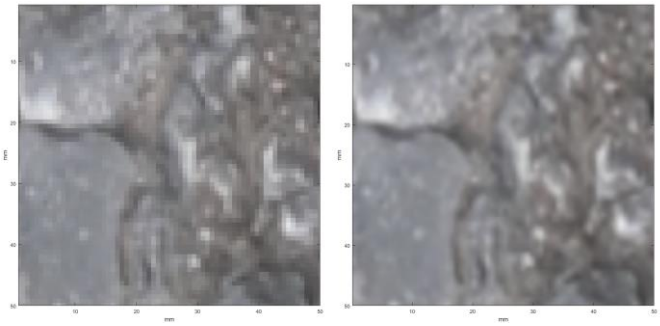

Figure 2. 5cm x 5cm patch of the asphalt texture model: original (left) and refined (right).

2. To enable real world applications of the system configuration with performance tested in synthetic simulations, the synthetic asphalt was scaled to have a middle level of average macrotexture MPD equal 0.83 mm. In this way, the target pavement shows realistic amplitude asperities over a large frequency range.

Using the Blender-Python API [7], gridded vertices, and triangulated faces of a mesh with displaced vertical coordinates is first created to represent the ground truth geometry of each synthetic pavement. Then, the generated 3D mesh is textured using a principle BSDF node in Blender, in which the base color and the light reflection roughness of the mesh surface are controlled and rendered using a physically based approach.

2.2 Rendering Synthetic Images

The length of the abstract is limited to 15 lines. The abstract should be self-contained and it must not refer to the other parts of the paper (such as the list of references). After the synthetic textured mesh of a pavement surface is created, an image acquisition plan including illumination condition and camera viewpoints is needed for optimization of tradeoff between spatial resolution and time/cost efficiency.

Optics. The critical parameters of a commercial off-the-shelf camera optics that influence the GSD of captured images on the target surface are: (a) the minimum focus distance, which is the closest capturing distance the camera can focus; (b) the depth of field (DoF), which is the vertical variability limit the survey can digitize. The reference project developed in the synthetic environment uses a virtual 4K camera of 30 mm focal length capturing at a height as low as 80-mm.

Macro camera lenses with a 1:1 or higher magnification ratio are widely used in applications of close-range photogrammetry [8]. The magnification ratio is the relationship of the size of a focused object in reality and the size of its reprojection on the camera image sensor. For a camera with pre-determined pixel size, a lens with higher magnification ratio enables capturing of images at a higher resolution. However, macro lenses exhibit a limited DoF without a time tedious process of focus stacking.

According to the size of image sensor, most commercial off-the-shelf cameras can be categorized into three types: micro-four thirds (17.3 mm x 13 mm), APS-C (about 23 mm x 15 mm), and full frame (36 mm x 24 mm). Figure 3 compares the three types of cameras and the relationship between GSD and DoF. The focal lengths are selected for individual camera type, so that they achieve same level of image GSD at an equivalent object (focus) distance. Although large image sensor size cameras feature superior performance in cases that require low-light (small aperture) and/or high-ISO settings, they result in shallower DoF assuming equivalent effective focal length. At a lateral resolution level of 10 μm, the three cameras produce DoF results of 4.44 mm, 3.12 mm, and 2.03 mm, respectively. Therefore, micro-four thirds camera type is selected in both the synthetic environment and the field experiments to achieve sufficient DoF with cost efficiency.

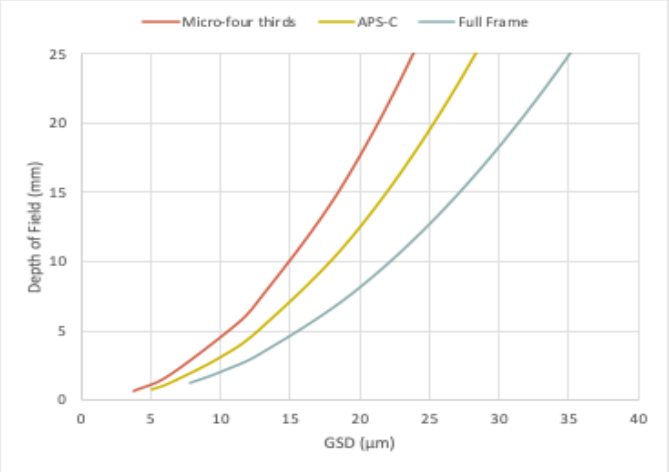

Figure 3. Depth of field (DoF) relationship with GSD for three camera types at a 60 mm equivalent effective focal length.

To capture full range of surface texture amplitudes in a targeting pavement, a DoF greater than the texture maximum height (S_z) is preferred. Most asphalt pavements have an MPD of less than 2 mm. Thus, a minimum GSD of 10 μm is selected for all configurations of image acquisition tested in the synthetic environment.

Scanning Area and GSD. The ground sampling distance (GSD) of captured images is a standard metric for the resulted spatial resolution of reconstructed point cloud, as it is the measured distance between two consecutive pixel centers on the ground. The determination of GSD depends on various factors including the camera focal length, the sensor pixel size, and the object distance (Figure 4a). A camera with fixed focal length captured at a higher height can result in larger GSD and lower spatial resolution (Figure 4b) compared to a closer range of photo capturing (Figure 4c). Ideally, a GSD is expected to be smaller than the smallest roughness horizontal scale to enable measurement of surface irregularities at the highest frequencies. However, the apparatus cost can be exponentially increased to have an image sensor with smaller pixel size and a macro camera lens that allows higher magnification ratio captured at a longer distance. While the synthetic environment is an effective tool enabling the use of simulated images "captured" by a virtual camera of any specifications at any distance, inevitable constraints on a low-cost field survey configuration should be taken into consideration.

DOI: 10.3217/978-3-99161-057-1-082

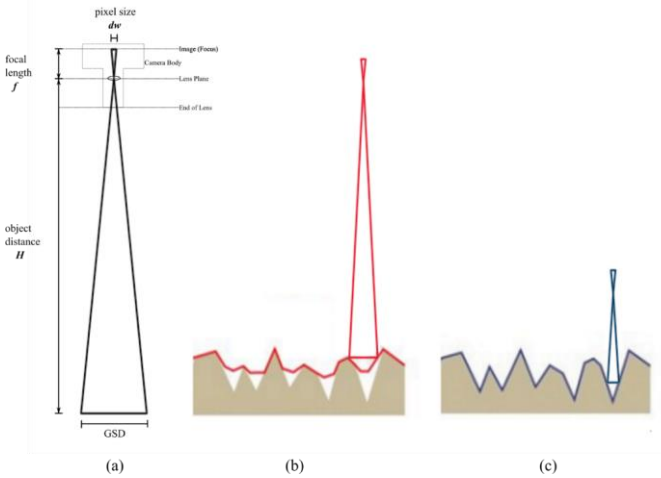

Figure 4. Determination of GSD (a), Large GSD – Low spatial resolution (b), and Small GSD – High spatial resolution (c).

Another factor that can affect the selection of GSD in a photogrammetric survey is the dimensions of target scanning area. A single 4K digital image can only capture about 16 mm in width if a 4 μm of GSD is used. Therefore, numerous numbers of images will be required for a single pavement texture 3D scan. This requirement can lead to tedious image acquisition work as well as long image processing time. Figure 5 shows the variation of the required number of images with GSD for a 3.77 μm pixel size 4K camera capturing a 120mm x 95mm surface area. The calculated number of required images include auxiliary images captured from multiple heights to ensure consistent mosaicking of partial scans. In the resolution range of 10 μm or smaller, the required number of images per survey is increased exponentially as GSD decreases. The minimum tested GSD of 10 μm enables not only enough DoF, but also reasonable image acquisition time. As the computational power grows and the cost per pixel decreases through time [9], the observed limitations can become negligible for future implementations.

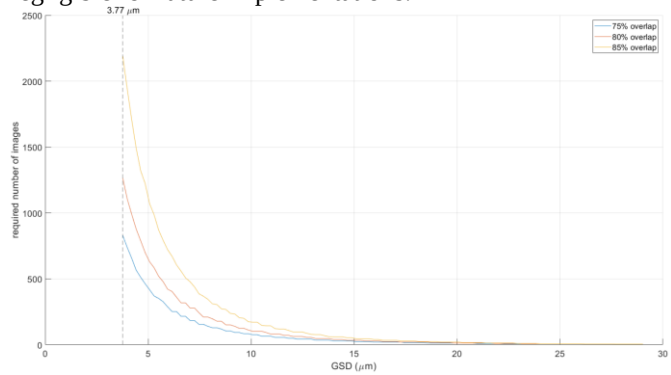

Figure 5. Required number of images with GSD for 4K camera scanning 120mm x 95mm area.

Scene and Lighting. The primary goal of lighting configuration is highlights while at the same time provide shadowless illumination. As discussed before, a camera with focus stacking technique may be needed if the aperture optimized for exposure provides insufficient DoF. In the proposed approach, fixed settings of F-stop (f/22) and ISO 200 are selected for deeper DoF and smaller visibility of noise. As the target object is partially insulated from the environmental illumination through set-ups including the surrounding control frame, close apparatus, and a very small aperture, a specific light source in conjunction with the sunlight is used towards proper exposure. In Figure 6, three images are rendered at 105 mm camera height with different energy settings of the added point light source. Therefore, proper adjustments of the light power output with object distance changes are required to prevent irreversible loss of data in the dynamic range.

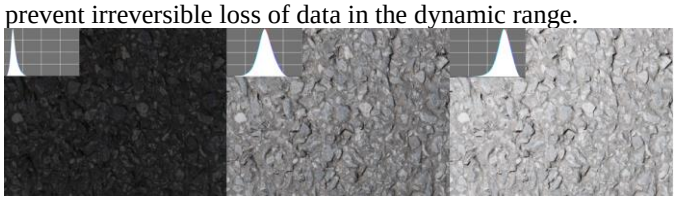

Figure 6. Synthetic rendered images of asphalt pavement texture with histogram at different light settings: (left) under exposed, (middle) proper exposure, and (right) over exposed.

Finally, a complete synthetic scene of pavement background and morning sunlight was used in image rendering processes. A 600mW power of diffused point light source moves along with the virtual camera is used to ensure shadowless and even imaging. In field studies, the shadow introduced by an imaging apparatus capturing at a close distance can be removed using a ring light installed around the camera lens. Figure 7 shows the rendered scene including a target object placed on the ground, a virtual camera facing down, and a diffused point light with pre-adjusted power output. Camera specifications and illumination configurations are set according to optimization of trade-off between cost, time, and resolution discussed in the above sections.

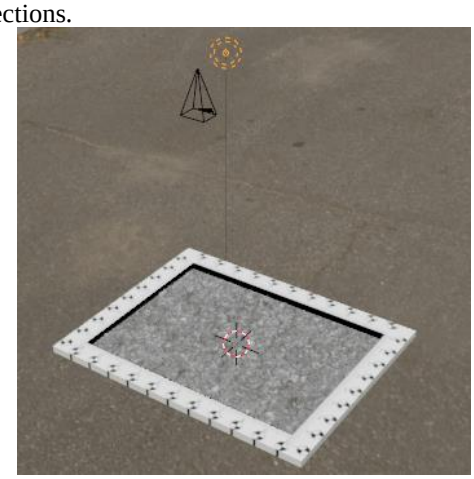

Figure 7. Scene and lighting configuration in synthetic environment.

Camera Motion. Images captured from numerous prescribed viewpoints are used in SfM technique to estimate the relative camera positions through feature matching, which is the start of triangulation processes. Both quantity and quality of the acquired images can greatly influence the feature detection performance. Following the principle of full coverage with high overlapping, two main strategies of shooting scenarios are widely used to obtain high quality of surface scanning: circular camera motion around the object, or viewpoints in a Cartesian lattice [8]. The former is preferred when the size of a single image footprint is greater than the target scanning area, whereas the latter is good for wider

DOI: 10.3217/978-3-99161-057-1-082

surface scanning. A minimum net scan area width of 100 mm is required for measurements of pavement macrotexture MPD. Therefore, one standard 4K image cannot fully cover a scanning area of the required size at a GSD smaller than 25 µm. However, the lowest wavelength of pavement roughness in rubber friction theory can be as small as a few micrometers [10]. This approach follows the Cartesian approach to avoid illumination artifacts and to achieve a lateral resolution as small as 10 µm. In addition, a few auxiliary images captured at larger heights are collected so that the overall reconstructed surface structure is consistent through small partial scans.

The accuracy of 3D reconstruction outputs and their performance in texture characterization are tested at multiple levels of GSD: 10 µm, 13 µm, 15 µm, and 38 µm in the developed synthetic environment. As shown in Figure 8, a Cartesian approach is used in the first three image acquisition plans as it allows closer object distance for smaller GSD. The strategy of circular camera motion around the target, at a 22.5◦ rotation interval, is also tested for comparison. The number of images used in the texturing of the reconstructed surface in four different image acquisition plans are 80, 35, 20, and 13, respectively. At least 80% image overlap is employed in all four plans since photogrammetry in a close-range scenario requires larger overlapping of images [11].

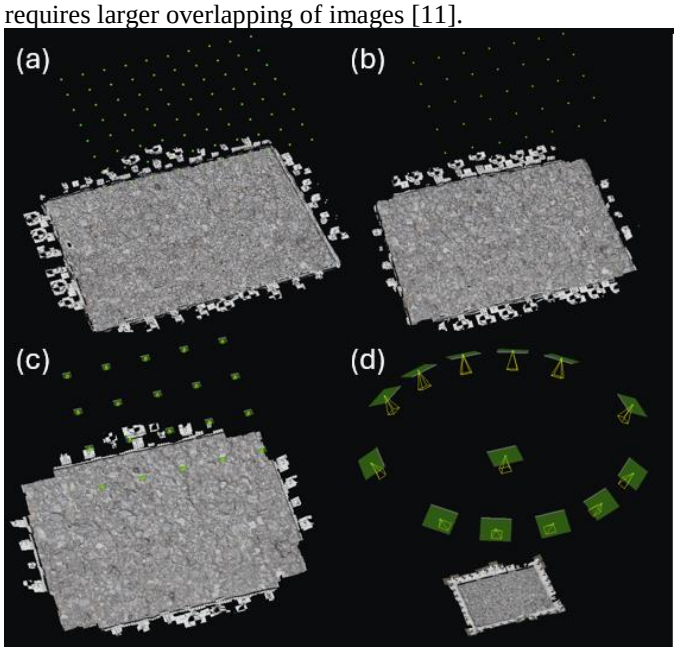

Figure 8. Image acquisition plans simulated in the synthetic environment tested at different GSD: (a) 10 µm, (b) 13 µm, (c) 15 µm, and (d) 38 µm.

2.3 Photogrammetric Process and 3D Reconstruction

All simulated images for each system configuration of pavement characteristics and camera viewpoints are imported in ContextCapture software [12] carrying out a photogrammetric process. The entire process includes three major stages: feature tracking, sparse reconstruction, and dense point cloud reconstruction.

First, the evenly distributed ground control points (GCPs) are detected in the images, either manually or automatically. An aerotriangulation process started from estimating the photogroup intrinsic and extrinsic properties. Taking into account the world coordinates of GCPs for georeferencing, the aerotriangulation detects and tracks matched features in the overlapped area of consecutive images. As a result, numerous automated tie points are detected and an estimation of camera properties is provided. Figure 9 shows an example of 4.412 tie points detected in one image "captured" at a GSD of 13 µm with a root mean square (RMS) reprojection error of 0.5 pixel. Enough tie points with sub-pixel parallaxes matched in the images is a good indicator of high precision in feature tracking.

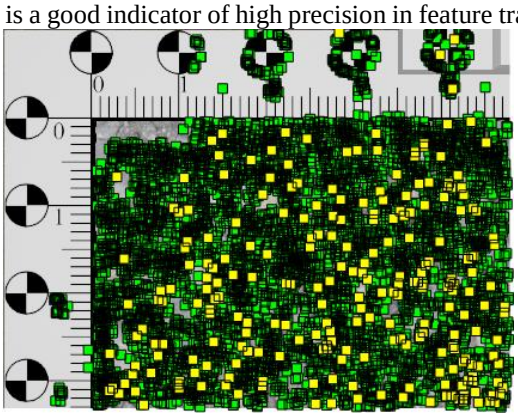

Figure 9. Example of 4,412 tie points detected in one rendered image by ContextCapture.

Next, the correspondence found between all tie points at the previous stage still contain errors and the camera pose estimates will be further refined in sparse reconstruction. At this stage, a bundle adjustment of camera internal and external parameters is employed for robust estimation. Taking advantage of redundancy in large number of detected tie points, this step estimates the geometry of the scene and obtains a sparse point cloud with robustness. Figure 10 shows the output of the sparse reconstruction stage of an asphalt surface texture modeled in the synthetic environment. The pavement model has an average MPD of 1 mm and was scanned at a GSD of 10 µm. The control frame on the edges is only used to provide GCPs and will not be included in the reconstruction of dense point cloud. This stage marks the end of SfM technique applications.

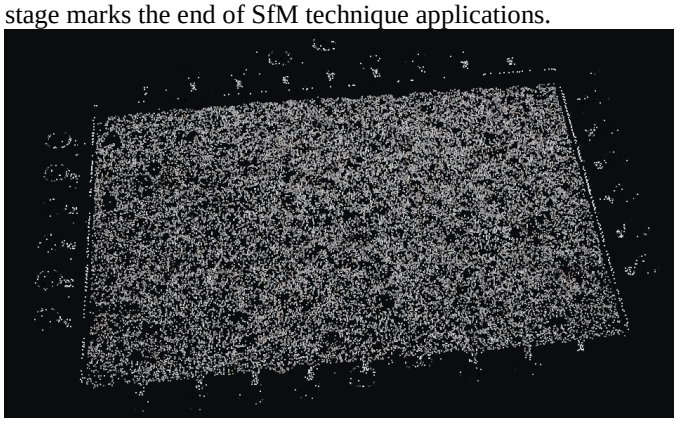

Figure 10. Sparse point cloud reconstruction output example.

The proposed photogrammetry approach requires a 3D reconstruction result of dense point cloud with a resolution equal or close to the determined GSD. Therefore, Multi-View Stereo is implemented to increase the point cloud density and reconstruct the 3D model with voxel color texturing according to stereo images of the scene captured with overlapping across different viewpoints. In both synthetic and laboratory

DOI: 10.3217/978-3-99161-057-1-082

environments, the camera motion can be controlled precisely with accurate positioning data. However, to simulate the outdoor scenario that camera positions are not available to be used as initial estimate of camera extrinsic parameters. In the proposed method, the scene coordinate system of a developed output 3D reconstruction was initialized using at least three arbitrary GCPs of choice instead. Figure 11 compares the top view of a synthetic asphalt surface in Blender and its 3D reconstruction model produced by ContextCapture at a spatial resolution of 10 μm. The original pavement model on the left is a mesh containing 1,567,362 vertices and 3,129,672 triangular faces. Due to the limited computational power (32Gb memory), the resulting resolution of the model is set as 24.41μm. Compared to the model ground truth, the 3D reconstruction on the right provides a top view picture with higher resolution. Although the two structures have different voxel resolutions, limited differences among the measurement of pavement texture parameters should be observed for a good photogrammetric texture reconstruction.

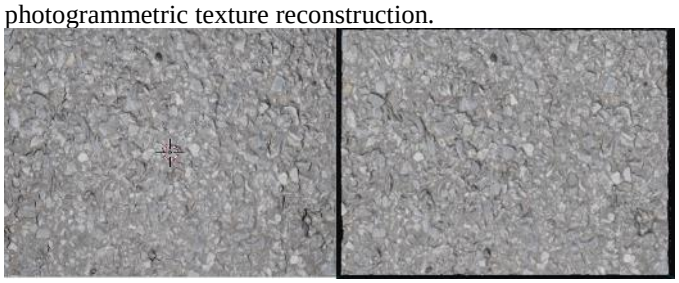

Figure 11. Synthetic asphalt pavement surface (left) and its 3D reconstruction with 10 μm spatial resolution (right).

3 DATA QUANTIFICATION AND EVALUATION

The quality of each photogrammetric survey can be assessed by quantifying the difference between ground truth and 3D reconstruction and its Digital Elevation Model (DEM).

3.1 3D Reconstruction Model Quality

Regardless of asperities in the surface topography, the modeling quality of a 3D reconstruction depends on the image acquisition plan, illumination, and camera intrinsic and extrinsic properties. Table 1 compares quality of 3D reconstruction outputs developed using different image acquisition plans. The density of the reconstructed point cloud remains uniform throughout the entire scanning area when a Cartesian approach is selected. Therefore, the resulted point cloud resolution of each Cartesian output is at the same level of the pre-determined image GSD (10 μm, 13 μm, and 15 μm, respectively). However, if a circular camera motion is selected, the resulted point cloud will be distributed at a range of resolution because of the inclined orientation of camera viewpoints. In this case, a sampling rate equal to the highest resolution (37 μm) or one pixel size (38 μm) will be used in the creation of surface DEM model even if smaller resolution values were observed in partial areas.

Generally, a large number of tie points per image with a sub-pixel parallax for images used in the aerotriangulation process is desired for high quality 3D reconstruction. The automated tie points detected in each image of the circular camera motion model (GSD=38 μm) is significantly decreased compared to results from the Cartesian approaches. A reason of this change is that the target surface was not covering the whole image footprint when the camera was capturing the entire object with a rotation in Z direction. An RMS reprojection error of less than one pixel size is observed for all four outputs, indicating that a satisfied precision in camera pose estimations can be obtained at various levels of point cloud resolution. As shown in Table 1, the average uncertainties found in estimation of image poses are less than 0.01 mm in all directions for three models with a GSD≤15 μm. For the model with 38 μm of GSD, the observed image pose uncertainties are also less than one pixel size for quality assurance. For all four model outputs, the image uncertainty in the Z direction is smaller than ones in the two horizontal directions, as the camera was moving mostly in the X and Y directions.

Table 1. Quality summary of 3D construction at different GSD levels in image acquisition/

Point Cloud Resolution Range	Median Tie Points per Image	RMS Tie Points Reprojection Error
0.0099 mm – 0.01 mm	4,541	0.55 pixels
0.013 mm	5,395	0.5 pixels
0.015 mm	6,025	0.5 pixels
0.028 mm – 0.037 mm	1,263	0.68 pixels

3.2 Digital Elevation Model Quality

Measurements of pavement texture only concern the height or elevation values of a target surface. Instead of conducting a direct comparison between voxels in two 3D structures, the 3D dense point cloud output of photogrammetry model will be rasterized to provide a surface DEM at one pixel sampling rate in MATLAB. The output map contains generalized height information of the input point cloud based on a local binning algorithm. As the GSD (one pixel size in mm) was selected as the fixed resolution of the grid element along X and Y axes, a few missing values are inevitable in the computed DEM and will be filled with linear interpolation. The corresponding percentage of the unfilled grids in DEM of the models with different grid resolutions are 0.099% (10 μm resolution), 0.1% (13 μm resolution), 0.15% (15 μm resolution), and 0.00056% (38 μm resolution) respectively. The number of unfilled grids in all four DEMs are neglectable compared to the matrix sizes. And the DEM of each 3D point cloud will be compared with the original displacement map of the synthetic asphalt pavement in terms of both residual errors and texture characteristics measurements. A visual comparison of the displacement (height) ground truth and the created model DEMs are displayed in Figure 12**.** According to the DEM surface plots, most of the height asperities of the structure are accurately scanned into the models. However, one deep pit was lost with a decreased absolute height in its 3D scans. The possible reason for this false is that occlusion happened when the optical paths were detecting the target point in valley.

DOI: 10.3217/978-3-99161-057-1-082

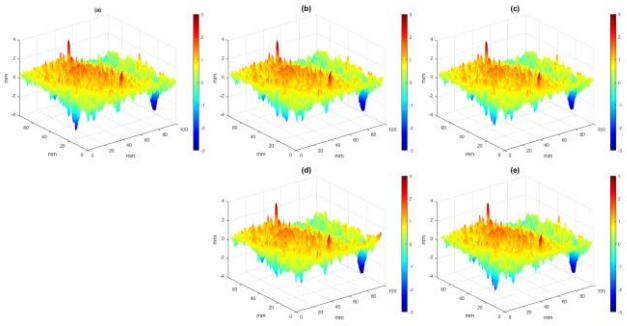

Figure 12. 3D surface plot comparison of surface ground truth (a) and DEMs of four 3D reconstructions of the synthetic pavement at different resolutions: 10 μm (b), 13 μm (c), 15 μm (d), and 38 μm (e).

Before comparing individual values in the ground truth matrix and the computed DEM of a 3D point cloud reconstruction, a spatial referencing process is needed to align the two matrices with different grid sizes. Then, the size of the matrix with a larger resolution is increased using linear interpolation. Finally, the residual errors of each DEM using the identical world coordinates are collected. Figure 13 shows the residual distribution of the DEMs compared to the ground truth. The shapes of residual histograms are close to normal distributions with zero means. It is observed that the RMS of all the residual distributions is within single digits of pixels. The general quality of a surface DEM is not improving with a decreased resolution. And the model sampled at 38 μm resolution provides the highest quality because a tilt camera view helped in preventing the occlusion issue. However, a high DEM general quality only means that the texture roughness in the range of wavelengths greater than 2 × resolution was reconstructed accurately. The height asperity data in higher frequency ranges of the original structure was lost.

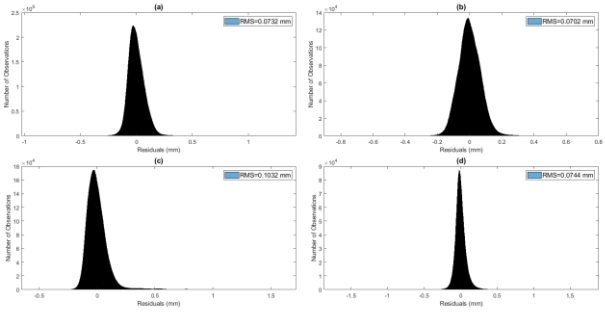

Figure 13. Residual distributions of DEMs of four 3D reconstructions of the synthetic pavement at different resolutions: 10 μm (a), 13 μm (b), 15 μm (c), and 38 μm (d).

After the spatial referenced comparison, the quality of a DEM needs to be further evaluated in terms of the characterization of pavement macrotexture and microtexture. To this end, a Butterworth filter was applied to both the pavement ground truth and the reconstruction DEMs to get: (iii) total texture roughness with wavelengths less than 50 mm, (ii) macrotexture with wavelengths within [0.5 50] mm, and (iii) microtexture with wavelengths ≤ 0.5 mm. Figure 14 illustrates the filtering process and its effects on the synthetic pavement ground truth. As shown in Figure 14d, the original synthetic pavement contains waviness with wavelengths greater than 50 mm and it will be filtered out before the texture characterization processes.

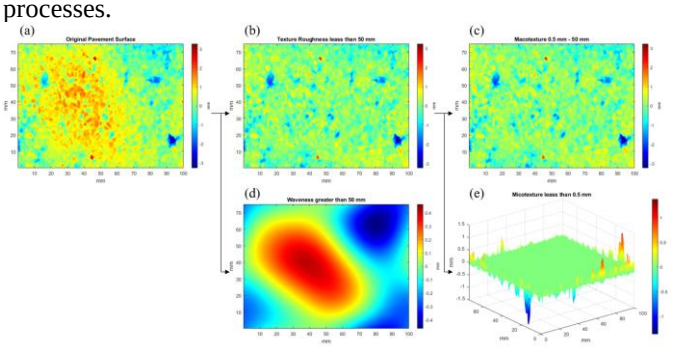

Figure 14. Butterworth filtering results on the synthetic pavement texture: (a) original surface; (b) total texture roughness; (c) macrotexture; (d) removed waviness; (e) microtexture.

3.3 Texture Characterization Quality

In this section, the macrotexture MPD and 3D areal parameters in total texture roughness measured from the 3D reconstructions will be evaluated.

First, the standard MPD is calculated from macrotexture of both the ground truth and the DEMs. Since different numbers of MPD measurements will be collected from data with different resolutions, the averaged MPD and the RMS MPD value will be compared as metrics. Since all four 3D reconstructions were sampled at a resolution much smaller than the microtexture lower bound wavelength (0.5 mm), the MPD measurements of DEMs are all accurate with small differences observed in the averages (<3.1%) and the RMS (<3%) compared to the ground truth, as shown in Table 2.

Table 2. Evaluation of the photogrammetric macrotexture MPD measurements.

Resolution	**Average MPD**		**RMS MPD**	
	mm	Diff (%)	mm	Diff (%)
Ground Truth	0.8305	-	0.8498	-
0.01 mm	0.8343	0.4596	0.8548	0.5910
0.013 mm	0.8048	-3.0875	0.8244	-2.9851
0.015 mm	0.8413	1.2991	0.8626	1.5069

Two pavements with the same macrotexture and microtexture amplitudes, e.g. MPD, can have different friction levels. A variety of supplemental variables have been used to represent the texture-friction correlation with improved performance. 3D areal parameters has been playing a significant role in tribological studies [13]. Adapted from the ISO 25178-3 [14] standard, a list of statistical quantitative texture measurements is used for comprehensive characterization of a 3D surface topography. Specifically, in total of 26 3D areal texture parameters were calculated across five categories: seven height parameters (arithmetic mean height ***Sa***, RMS height ***Sq***, minimum peak height ***Sv***, maximum peak height ***Sp,*** skewness ***Ssk***, and kurtosis ***Sku***), two hybrid parameters (root mean square gradient ***Sdq*** and developed interfacial area ratio ***Sdr***), three spatial parameters (autocorrelation length Sal, texture aspect ratio ***Str***, and the texture direction in rad Std), five

DOI: 10.3217/978-3-99161-057-1-082

feature parameters (the density of peaks ***Spd***, arithmetic mean peak curvature ***Spc***, five-point peak height S_{5p} five-point pit height, S_{5v}, and ten-point surface height, S_{10z}), and nine functional parameters (peak material volume ***Vmp***, core material volume ***Vmc***, core void volume ***Vvc***, dales void volume ***Vvv***, peak extreme height ***Sxp***, surface section difference ***Sdc***, reduced peak height ***Spk***, core height Sk, and reduced dale height ***Svk***).

The measurements of all seven height parameters were robust among four 3D models. The differences between the 3D measurements and the ground truth are less than 5%.

The two hybrid parameters are both good indicators of texture roughness in general. As Sdq increases, the surface is inclined steeply. The surface becomes more rough when the Sdr value increases. All three 3D models with a resolution smaller than the ground truth resolution (24.4 μm) provide good measurements of the hybrid parameters. However, significant errors (>10% difference) are observed for the model that has a larger resolution (38 μm).

Spatial parameters measure the surface horizontally. Therefore, the accuracy of 3D measurements varies depending on the influence of surface isotropy in the high frequency range. The strongest surface orientation was not accurately detected in the two 3D models of higher resolution (15 μm, 38 μm).

Due to the sensitive nature of feature parameters, the difference observed between the ground truth and the 3D measurements in this category are large. Among the four 3D reconstructions, the circular camera motion model with a resolution of 0.038 mm has the best performance in feature parameters measurements. The reason is that a tilt camera orientation can help in capturing the actual value of points with the largest global peaks and pits heights. However, there is a trade-off between the sampling resolution and camera orientation. Therefore, feature parameters will not be used in the friction prediction modeling process utilizing the field texture measurements.

Most of the nine functional parameters are measured accurately in the four 3D models. Some error in Vmp measurement were observed in two models with the smallest resolutions (10-μm and 13 μm). A possible reason is that redundant volume of extreme peaks are sampled in the two models as the result of linear interpolation. The significant differences in Spk and Sxp measurements for the 3D model with 15 μm indicate that this model failed to scan some peak height values.

4 FIELD EXPERIMENT

A low-cost commercial off-the-shelf camera (Lumix GX850) with a micro-four thirds 4K image sensor (4592×3448) installed with a macro lens is utilized in the field capturing images of pavement surface texture. The selected macro lens has a fixed focal length of 30 mm and a minimum focus distance of 105 mm (equivalent to a minimum working distance of about 22 mm). To minimize shake and achieve a spatial resolution of the order of tenth of micrometer, the camera was mounted on a tripod with a working height as low as 55 mm. In addition, a 180 mm rail nodal slider is fitted on the tripod to ensure consistent overlapping between consecutive images. Although the macro lens allows a maximum magnification ratio of 1:1, a smaller magnification (1/3) is selected to allow larger DoF at f/22 aperture. The target three track roads have previous MPD measurements fall in the range of 0.1 mm – 2 mm. Therefore, a DoF of 5.63-mm should be sufficient to capture the asperities in amplitudes. As tested in the synthetic environment, a battery powered ring light is added to compensate for the low environmental lighting resulted from the shallow aperture.

A LTS measurement pair for each photogrammetric texture scans was recorded for initial validation purposes of field MPD measurements. The LTS Model 9200 by Ames scans enables selected number of 100 mm length 2D texture profiles at a horizontal resolution of 0.015 mm. The device needs approximately 15 minutes to complete 50 scans of profiles over a scan area of 107.95 mm by 72.01 mm.

Figure 15 shows all the apparatus utilized in field texture measurements as well as the LTS used for validation purposes. The total cost of all equipment listed in Figure 15b is less than $1000. Specifications of the photogrammetry device used for field texture scan are listed in Table 3.

Figure 15. Apparatus of field texture scans: (a) LTS model 9200, (b) 4K camera, macro lens, tripod, slider, and ring light.

Table 3. Summarized specifications of texture scan using LTS and photogrammetry.

SfM-based Photogrammetry	
Total scan area	100 mm × 75 mm
Resolution	0.011 mm in X, Y, Z directions
Pixel Size	3.77 μm
Image Sensor Size	17.3 mm × 13 mm (4592×3448)
Aperture	f/22
ISO	200
Focal Length/GSD	30 mm/0.011 mm

Field data collection of pavement friction and texture was conducted on three track roads in Spring 2024. As shown in Figure 16, the research and development division of INDOT has three track pavements with distinct MPD levels: two hot-mix asphalt (HMA) pavements at the left and middle lanes, and one slick concrete pavement on the right. For each road, two longitudinal sections (each about 65 feet long) along with three locations: the left wheel-path, the center line, and the right wheel-path were selected as individual test locations. The three transversal locations are assumed to have different levels of traffic polishing. Consequently, the difference observed in friction data gathered from the three locations within each road will explain the influence of traffic polishing on road wet friction performance. On the other hand, two longitudinal sections for each road were selected for data argumentation,

DOI: 10.3217/978-3-99161-057-1-082

assuming that the pavement surface texture in real world is not homogenous in real-world scenarios.

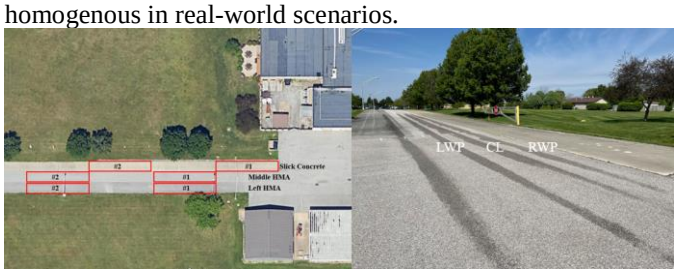

Figure 16. The test fields: three track roads in INDOT. Each road includes two longitudinal sections (left) and three transversal locations (right).

After texture data collection, a LWST was employed to obtain the pavement friction number (FN) at two vehicle speed levels with multiple repetitions. In total of 130 LWST measurements were completed in three days, and the test temperature of pavement varies between 45°F to 112°F.

The residual errors of GCPs during the reconstruction of the field surfaces increases compared to the synthetic test results. One important reason is the additional uncertainties caused by calibration of a real-world camera with lens distortion. To verify the method reliability in the field, a comparison of macrotexture MPD measurement distributions between the proposed photogrammetric method and its LTS counterpart is employed. Since the measurement sampling rates and locations in the transversal direction varies, two sample T tests are employed to compare the average MPD in the distributions provided by the two methods. All 41 tests failed to reject the null hypothesis that MPD measured by photogrammetry and LTS are from populations with equal means at a 5% significance level.

The R-square value of 0.7672 indicates that limited information in the road friction performance can be explained by the standard macrotexture MPD solely. Therefore, three alternative models are trained: stepwise linear regression, neural network (NN) model, and regression ensemble model (random forest). The optimized regression ensemble model contains 47 learners of all 25 predictors. And the model achieves better goodness-of-fit compared with both the stepwise linear model and the NN. As shown in Table 4, a R-squared (Test) of 0.98 is obtained. The RMSE (Test) has been reduced to 3.36, and the MAE (Test) is only 2.55. It is worth noting that the MAE statistic (mean absolute error) is less sensitive to outliers compared to RMSE and MSE.

Table 4. Performance of three texture-based FN prediction models.

Model	RMSE (Valid)	R-squared (Valid)	RMSE (Test)	R-squared (Test)
Stepwise LR	4.853	0.960	4.995	0.956
Neural Network	5.318	0.952	4.796	0.959
Ensemble	3.549	0.978	3.361	0.980

As discussed in the synthetic simulations, a selection of small image GSD leads to high spatial resolution in the 3D photogrammetric pavement texture reconstruction. Consequently, the measurement quality of texture roughness characteristics is also changed with the sampling rate. The comparison results of an asphalt pavement surface scanned at multiple image GSD in the synthetic environment suggest that a DEM developed using the proposed 3D reconstruction method with a GSD/resolution of 0.011 mm – 0.013 mm can provide reliable measurements of 23 distinct texture parameters, as long as the maximum imaging DoF is sufficient for feature capturing of extreme peaks and pits. However, the highest frequency of pavement microtexture is undefined. Therefore, the minimum spatial resolution in surface texture scan required for reliable prediction of pavement friction performance is still debated.

The original 3D reconstruction of 41 field texture photogrammetric scans will be down sampled at a scale of 0.5 multiple times. Next, texture DEMs of the down sampled point cloud data are developed, among which there are five distinct resolution levels: 0.022 mm, 0.044 mm, 0.088 mm, 0.176 mm, and 0.352 mm. The 22 areal texture parameters are measured using the down sampled texture DEMs. The original speed, pavement temperature, and macrotexture MPD are kept as they were not affected by the down sampling process. Finally, new observations with changed values in 22 texture predicators are collected.

The optimal regression ensemble model is used to predict FN using the six test groups of data observations. The prediction performance in terms of resolution changes is measured using the test RMSE and R-squared values. High R-squared values are observed in test results of all five samples, indicating that most of the pavement performance can be explained by pavement macrotexture. However, the RMSE between predicted FN using input of 25 predicators and the true FN provided by a LWST increases as the spatial resolution in texture 3D scan increases. Therefore, the texture asperities at micro-scales have contributed to the friction performance of a pavement surface. According to the increasing rates of test RMSE shown in Figure 17, it is suggested that the spatial resolution of a comprehensive 3D texture scan for friction prediction should be smaller than 0.1 mm at the least.

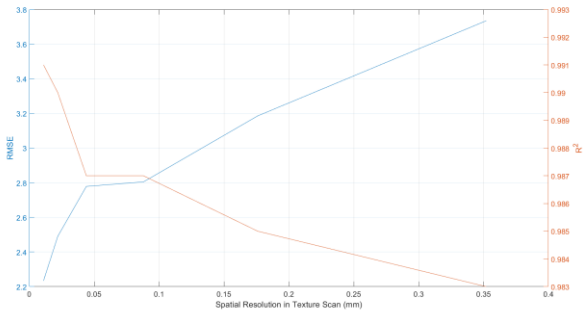

Figure 17. Relationship between the Model performance and spatial resolution in texture scans.

5 CONCLUSION

This paper develops a prototype of image-based pavement texture measurement for friction prediction in a non-contact manner. Towards the goal of data quality assurance, a synthetic environment is developed before field implementation. The

DOI: 10.3217/978-3-99161-057-1-082

survey simulations evaluate sensitivities in texture measurements arising from different experimental designs and testing feature configurations. The minimum condition for optimized 3D surface reconstruction of pavement surface is discussed. Finally, a field experiment investigates the characterization of surface texture at different scales and their contribution to pavement friction performance.

ACKNOWLEDGMENTS

The authors would like to thank Michael Sanders of INDOT for his input and technical guidance in the field road friction experiments.

REFERENCES

[1] S. Li, S. Noureldin, and K. Zhu, "Safety Enhancement of the INDOT Network Pavement Friction Testing Program: Macrotexture and Microtexture Testing Using Laser Sensors," 2010. doi: 10.5703/1288284314248.

[2] M.-T. Do and V. Cerezo, "Road surface texture and skid resistance," *Surf. Topogr.: Metrol. Prop.*, vol. 3, no. 4, p. 043001, Oct. 2015, doi: 10.1088/2051-672X/3/4/043001.

[3] M. S. Nielsen, I. Nikolov, E. K. Kruse, J. Garnæs, and C. B. Madsen, "Quantifying the Influence of Surface Texture and Shape on Structure from Motion 3D Reconstructions," *Sensors*, vol. 23, no. 1, Art. no. 1, Jan. 2023, doi: 10.3390/s23010178.

[4] P. Martínez-Carricondo, F. Agüera-Vega, F. Carvajal-Ramírez, F.-J. Mesas-Carrascosa, A. García-Ferrer, and F.-J. Pérez-Porras, "Assessment of UAV-photogrammetric mapping accuracy based on variation of ground control points," *International Journal of Applied Earth Observation and Geoinformation*, vol. 72, pp. 1–10, Oct. 2018, doi: 10.1016/j.jag.2018.05.015.

[5] D. S. Dharshan Shylesh, N. Manikandan, S. Sivasankar, D. Surendran, R. Jaganathan, and G Mohan, "Influence of quantity, quality, horizontal and vertical distribution of ground control points on the positional accuracy of UAV survey," *Appl Geomat*, vol. 15, no. 4, pp. 897–917, Dec. 2023, doi: 10.1007/s12518-023-00531-w.

[6] ambientCG, "ambientCG - CC0 Textures, HDRIs and Models." Accessed: Apr. 14, 2024. [Online]. Available: https://ambientCG.com/

[7] Blender, "Blender 4.1 Python API Documentation." Accessed: Apr. 16, 2024. [Online]. Available: https://docs.blender.org/api/4.1/#

[8] P. Koutlemanis, X. Zabulis, N. Stivaktakis, N. Partarakis, E. Zidianakis, and I. Demeridou, "A low-cost close-range photogrammetric surface scanner," *Front. Imaging*, vol. 3, Jan. 2024, doi: 10.3389/fimag.2024.1341343.

[9] Q. Alexander, V. Hoskere, Y. Narazaki, A. Maxwell, and B. Spencer, "Fusion of thermal and RGB images for automated deep learning based crack detection in civil infrastructure," *AI in Civil Engineering*, vol. 1, Aug. 2022, doi: 10.1007/s43503-022-00002-y.

[10] B. N. J. Persson, "Theory of rubber friction and contact mechanics," *The Journal of Chemical Physics*, vol. 115, no. 8, pp. 3840–3861, Aug. 2001, doi: 10.1063/1.1388626.

[11] G. Guidi, U. Shafqat Malik, and L. L. Micoli, "Optimal Lateral Displacement in Automatic Close-Range Photogrammetry," *Sensors*, vol. 20, no. 21, p. 6280, Nov. 2020, doi: 10.3390/s20216280.

[12] Bentley, "iTwin Capture Modeler | Bentley Systems | Infrastructure Engineering Software Company." Accessed: Apr. 16, 2024. [Online]. Available: https://www.bentley.com/software/itwin-capture-modeler/

[13] L. A. Franco and A. Sinatora, "3D surface parameters (ISO 25178-2): Actual meaning of Spk and its relationship to Vmp," *Precision Engineering*, vol. 40, pp. 106–111, Apr. 2015, doi: 10.1016/j.precisioneng.2014.10.011.

[14] ISO, "ISO 25178-3:2012," ISO. Accessed: Oct. 14, 2024. [Online]. Available: https://www.iso.org/standard/42895.html